ELSEVIER

Polymer 41 (2000) 511–522

polymer

Gas-sorption effects on plasma polymer films characterized by XPS and quartz crystal resonator

I. Sugimoto*, M. Nakamura, N. Kasai, T. Katoh

NTT Lifestyle and Environmental Technology Laboratories, Midori-cho, Musashino-shi, Tokyo 180-8585, Japan

Received 2 April 1998; received in revised form 19 August 1998; accepted 24 February 1999

Abstract

The fundamental gas-sorption properties of sputtered polymeric films (fluoropolymer and amino acid films) are clarified using a quartz crystal resonator as a film substrate of a piezoelectric mass transducer. X-ray photoelectron spectroscopy suggests that the surface molecular structure of the fluoropolymer film does not change after the sorption of oxygen and fluorocarbon gases. Sorption measurements in a vacuum chamber show that the fluoropolymer film completely releases the residual gas even at a low vacuum (8×10^{-2} Torr) and softened by the increase of temperature, whereas, the D-phenylalanine film does not completely emit the sorbed gas even at a high vacuum (5.5×10^{-7} Torr). The fluoropolymer film retains its solvent characteristics without changing its mechanical properties for non-polar organic gases under saturated vapor conditions; however, damping occurs in polar organic gases along with bond formation. The concentration-dependence of sorption capacities for chlorinated ethylenes and benzene derivatives classifies the amino acid film as a polar solvent or the PCTFE film as a non-polar solvent.

Keywords: Plasma polymer film; Radio-frequency sputtering; Gas-sorption

1. Introduction

Plasma polymer films inevitably contain unsaturated carbon moieties (multiple bonds and radical sites) [1]. These unsaturated carbon moieties in polymeric carbon networks can interact with small organic molecules by means of π-electrons and unpaired electrons. In addition, the unsaturated radical sites in carbon networks are likely to enhance the mobility of highly cross-linked carbon networks [2], making them effective at solvating small organic molecules. These promising structures suggest that plasma polymer films can behave as good solvents for any type of solute.

The gas-sorption behaviors of polymeric films directly reflect how they interact with solute gas molecules and thus offer information about the structure of the solvent polymer films. The sorption capacity [corresponding to partition coefficient (K)] of solvent polymer films can be assessed by thermodynamic and physicochemical analysis of solute/solvent intermolecular interactions. The linear solvation energy relationships (LSERs) [3–5] are one of the most successful solvation concepts to quantitatively describe the sorption capacity:

$$\log K = C_0 + r(R_2) + s(\pi_2) + a(\beta_2) + b(\alpha_2) + l(\log L_{16}),$$

where C_0 is a regression constant; and $r(R_2)$, $s(\pi_2)$, $a(\beta_2)$, $b(\alpha_2)$, and $l(\log L_{16})$ are measures of the polarizability of the solvent film (of the solute gas), the polarity, the hydrogen-bonding acidity (basicity), the hydrogen-bonding basicity (acidity), and the dispersion/cavity (represented by Ostwald coefficient [6]) factors, respectively. None of these terms is completely independent of the others; the polarity is somewhat correlated with the acidity and basicity of hydrogen-bonding, and the polarizability and polarity are linked with the dispersion factor for solvation. The LSERs can offer a guiding principle for understanding and designing solvent polymeric films for use in sorption, separation and sensing layers.

However, complete uniformity of the film structure is required to verify these LSERs. In practice, a film structure may change with depth, which frequently occurs in plasma products. The longitudinal region of the solvent film can be roughly divided into three zones: the vicinity of the film/substrate interface, the bulk and the surface. Considering the gas-sorption mechanism in detail, the surrounding gas molecules first adsorb and migrate on the surface of the polymeric film and then diffuse into the subsurface region and then the bulk of the solvent film. This diffusion process

* Corresponding author. Tel.: +81-422-59-2635; fax: +81-422-59-3427.
E-mail address: sugimoto@ilab.ntt.co.jp (I. Sugimoto)

0032-3861/00/$ - see front matter
PII: S0032-3861(99)00192-5

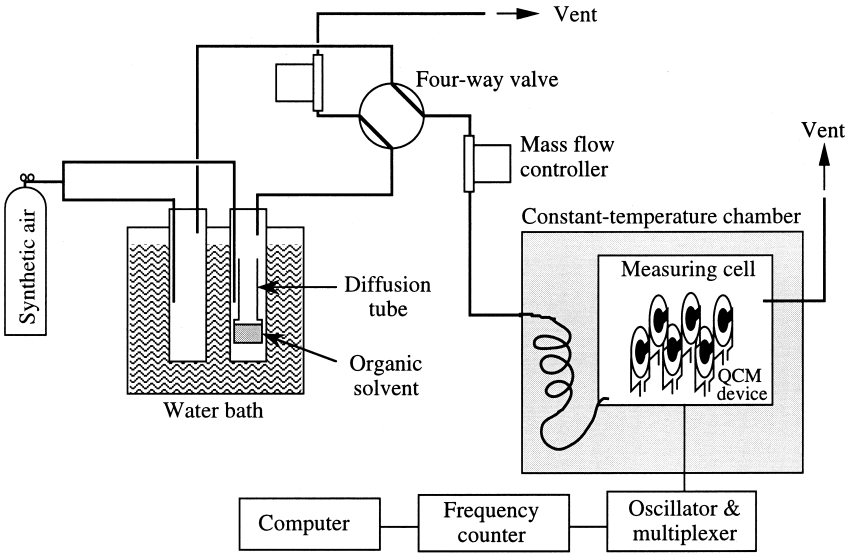

Fig. 1. Gas sorption measurement system for volatile organic compounds.

proceeds until the solvation capacity is maximum, attaining the sorption/desorption equilibrium state. To analyze in detail, we should interpret the adsorption/absorption behavior of the solute gas and solvent film corresponding to the aforementioned regional and phenomenological differences.

A quartz crystal resonator (QCR) is a well-established piezoelectric mass transducer, which can measure mass changes smaller than the nanogram order [7,8]. The QCR method is rugged and versatile, and can detect the mass loading on the resonator either in the gas or liquid phase. The superior linearity between the changes in resonance frequency and in loaded mass is also attributable to the wide range over which the QCR can be used as a sensitive chemical sensor and film-thickness monitor. This QCR device is also effective for monitoring specific reactions, such as biological and acid–base reactions.

This article reports the fundamental gas-sorption behavior of the plasma polymer films, which are produced by radio-frequency sputtering of either fluoropolymers or amino acids. The basic gas-sorption analysis is performed in a vacuum chamber, in which the structural information can be obtained under well-controlled pressure and temperature. We also discuss the solvation capability of the solvent films for solute organic gases on the basis of physicochemical molecular descriptors, such as dipolarity and polarizability, which are decisive factors in LSERs.

2. Experimental

2.1. Preparation of plasma polymer films

The plasma polymer films were produced using a diode-type radio-frequency (rf) sputtering apparatus equipped with an ultraviolet (UV) light irradiation system [9,10]. A polychlorotrifluoroethylene (PCTFE) disk (135 mm in diameter, 10 mm thick) was used as a sputtering target. Ar was introduced into the plasma chamber at 5 ml/min, and the rf power was applied to the lower electrode with a mean density of 1.12 W/cm^2. The sputtered polymer film was deposited on a 9 MHz AT-cut quartz crystal plate (8.5 mm in diameter and 0.1 mm thick) for gas-sorption measurements, and on a ⟨100⟩ non-doped silicon wafer for the spectroscopic analysis. These film substrates were placed on the upper grounded electrode; the interelectrode distance was 55 mm.

We previously reported that the formation of unsaturated bonds can be enhanced by UV light irradiation during the rf sputtering of fluoropolymer films because the atomic bonds in the film constituents are cleaved by photo-excitation [11]. This sputtering technique can increase the π-electron density and the spin-density in the resulting fluoropolymer films. To enhance photo-excitation, during sputtering deposition, UV light (185 and 254 nm) was irradiated over the whole volume of the plasma by a 300 W low-pressure mercury lamp through a CaF_2 window. We refer to this UV-light-irradiated sputtering as *photo-assisted sputtering*. In turn, sputtering without UV light irradiation is referred to as *conventional sputtering*.

Amino acid films were also produced by rf sputtering, and the film-deposition procedure was similar to that previously reported [12]. D-phenylalanine, D-tyrosine and D-glutamic acid (>98%) were obtained from Tokyo Kasei and Kanto Chemical and used without further purification. Each amino acid was suspended in ethanol at 70°C and the dispersed solution was spread on the polyethylene disk. We then used the polyethylene disk coated with amino acid as a sputtering target after the ethanol was fully evaporated. To minimize the decomposition of amino acids induced by sputtering effects, we used He as a plasma-working gas. The gas pressure during sputtering was 1.7×10^{-2} Torr and the rf power density was 0.42 W/cm^2.

Table 1
Molecular descriptors of volatile organic compounds (VOCs)

VOCs	Dipole moment (debye)	Polarizability ($\times 10^{-24}$ cm^3)	Tracks activity (P/P_0[a], $\times 10^{-5}$)	Heat of vaporization (kcal/mol)
Dichloromethane	1.36	3.31	3.80	7.52
Chloroform	1.02	4.77	7.79	7.50
Carbon tetrachloride	0.00	6.34	14.48	7.63
Tetrachloroethylene	0.00	7.82	84.44	9.24
Trichloroethylene	0.47	6.23	20.54	8.31
cis-1,2-dichloro-ethylene	1.10	4.66	7.68	7.42
trans-1,2-dichloro-ethylene	0.00	4.85	4.78	7.24
Methanol	1.59	1.58	11.98	9.38
Ethanol	1.40	2.65	25.69	9.67
n-propanol	1.44	3.71	74.22	10.86
n-butanol	1.40	4.75	235.29	10.97
n-pentanol	1.39	6.84	697.25	12.50
n-heptanol	1.42	7.89	6608.70	13.92
n-hexane	0.02	6.34	7.98	7.63
n-heptane	0.02	7.38	33.25	8.67
n-octane	0.02	8.43	108.73	9.22
Cyclohexane	0	6.20	15.58	7.83
Benzene	0	6.76	15.97	9.20
Toluene	0.26	8.01	53.46	8.76
o-xylene	0.44	9.26	230.30	10.00
m-xylene	0.44	9.26	183.13	9.90
p-xylene	0.05	9.33	173.52	9.81
Ethylbenzene	0.30	9.10	159.86	9.30
Chlorobenzene	0.95	8.17	162.98	9.59
Acetone	2.78	3.64	6.57	7.64
2-butanone	2.66	4.69	16.82	8.15
2-hexanone	2.66	6.78	118.20	12.36
Methylacetate	1.82	4.25	7.02	7.73
Ethylacetate	1.89	5.40	156.99	8.30
N,*N*′-dimethylformamide	3.46	4.94	410.81	—
Cyclohexanol	1.47	6.66	1125.93	11.94

[a] P/P_0 represents the condensation ability and the resulting loss of the free vapor state: P = partial pressure (20 ppm), P_0 = saturation vapor pressure at measurement temperature (25°C).

The plasma-organic film thickness deposited on each side of the quartz crystal plate was controlled to be approximately 0.5 μm, which was determined from the difference in the resonance frequency of the QCR before and after deposition.

2.2. X-ray photoelectron spectroscopy (XPS)

The X-ray photoelectron spectra were obtained using a VG ESCALAB-MK2 spectrometer, with Mg-Kα radiation at 300 W used as the X-ray excitation source. The prepared fluoropolymer samples were stored in a vacuum desiccator at $<1\times10^{-1}$ Torr to prevent aging and contamination; the time interval between film preparation and XPS measurement was less than three days. The chamber pressure during analysis was kept at $<4\times10^{-10}$ Torr and ion-etching to remove surface contamination was not carried out to avoid any structural changes. The incident angle of the X-ray beam and the photoelectron take-off angle with respect to the film surface were 40° and 90°, respectively. Each binding energy was calibrated to compensate for charging by setting the F1s peak to 689 eV, which is characteristic of fluoropolymers [13].

2.3. Gas-sorption measurements and evaluation of sorption capacity

The set-up we used to measure the sorption capacity of the fluoropolymer-coated QCR devices is shown in Fig. 1. The solute gases were generated from a liquid solvent contained in a diffusion tube immersed in a temperature bath. Synthetic air (99.9999% pure) was used as both the carrier gas and the standard gas for establishing the initial state. Commercial organic solvents for generating the volatile organic compound (VOC) stream were used without further purification (>98% pure). The gas concentration was controlled by adjusting the temperature of the diffusion tube between 30 and 50°C; the flow rate of the carrier gas was 0.2 l/min in most cases. The film-coated QCR was attached to an oscillator circuit and placed in a 30 ml aluminum measurement cell, which was in a chamber kept at a constant temperature of 25°C. The VOC stream was introduced into the measurement cell after its baseline

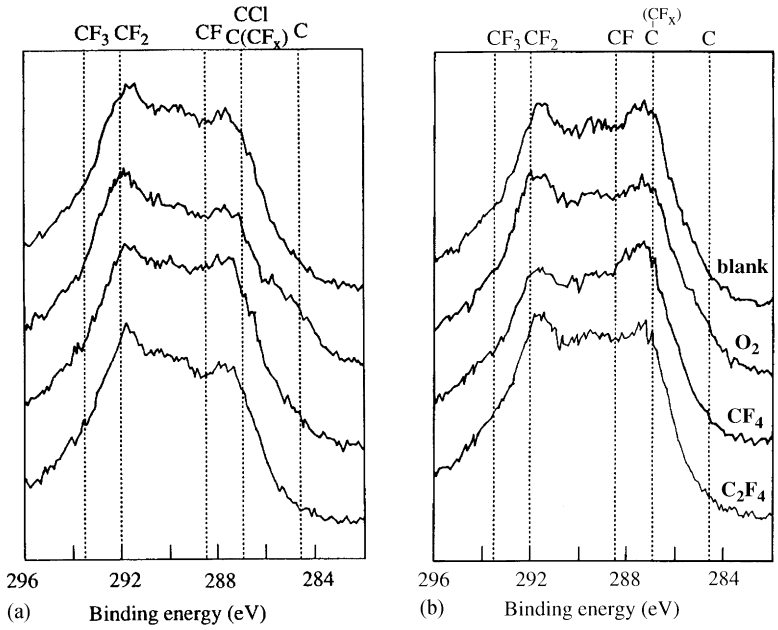

Fig. 2. C1s-XPS spectra: (a) before; and (b) after gas sorption.

fluctuation had been suppressed to below 0.1 Hz/min. Switching between the background- and measurement-modes was done quickly by using a four-way valve, which produced a step response and kept the gas pressure constant before and after switching. The sorption capacities were determined by the frequency changes after three hours of sorption measurements. We used Sauerbrey's [14] to relate the frequency change (Δf) to the mass loading (Δm):

$$\Delta m = -[A(\rho_q \mu_q)^{1/2}/2F_0^2]\Delta f,$$

where F_0 is the fundamental frequency of the unloaded QCR (9 MHz), A is the electrode area (0.13 cm^2), ρ_q is the density of quartz (2.65 g/cm^3), and μ_q is the shear modulus of quartz (2.95×10^{11} dyne/cm^2). With these constants, we obtain

$$\Delta m(\text{ng}) = -1.05\Delta f(\text{Hz}).$$

The frequency shifts obtained by changing the pure air stream through the background line to the other pure air stream through the gas generation cell without the gas source installed were less than 0.3 Hz. The accuracy of frequency measurement was 0.1 Hz.

The impedance analysis was performed by using an HP-4195A network/spectrum analyzer. The film-coated QCR connected to an impedance test adapter (HP 41951-69001) was exposed to the closed headspace of VOC in a 100 ml flask kept at 25°C.

2.4. Molecular descriptors for intermolecular interaction

We obtained the dipole moments and polarizabilities (Table 1) by establishing energy-minimized molecular structures by using molecular mechanics (MM2) [15] and molecular orbital packaging (MOPAC) [16], both included in CAChe molecular modeling software (Sony-Tektronics) running on a Macintosh Quadra-800™ system. Both molecular descriptors of VOCs can be informative parameters to analyze the intermolecular interactions. We list these descriptors of typical VOCs in Table 1, which also shows two other important characteristics of VOCs: the tracks activity (20 ppm at 25°C) and the molar heat of vaporization [17], which can be a measure of the self-association abilities of VOCs.

3. Results and discussion

The surface structural changes induced by the inorganic gas-sorption were examined by XPS, which used the solute gas as a molecular probe. We measured the spectra before and after sorption of O_2 and fluorocarbon (CF_4 and C_2F_4) gases (at 760 Torr for 1 h). We used these gases as molecular probes because they are considered to be the most detectable species if chemical bond formation with solvent film occurs. This is because the fluorinated and oxygenated moieties in the film molecules induce large chemical shifts due to their inductive effects, resulting in prominent features in the C1s-XPS spectra.

Comparison of the C1s-, F1s- and Cl2p-XPS spectra before and after gas-sorption gave a straightforward identification of their structures. As shown in Fig. 2, all of the XPS measurements after gas-sorption indicated changes in the C1s-XPS spectra: the signal intensity of the lower binding energy at 287.5 eV increased and that of the higher binding energy at 292 eV decreased. However, this tendency was also observed for the blank test, in which gas-sorption was not implemented between first and second measurements.

Table 2
Atomic ratios of film components evaluated by XPS

Element	Sorption	Concentration (%)		Ratio (C_b/C_a)
		Before sorption (C_b)	After sorption (C_a)	
Carbon	Blank	49	51	1.04
	O_2	50	51	1.02
	CF_4	50	52	1.04
	C_2F_4	47	50	1.04
Fluorine	Blank	37	36	0.97
	O_2	35	36	1.03
	CF_4	34	34	1.00
	C_2F_4	38	38	1.00
Chlorine	Blank	13	12	0.92
	O_2	15	12	0.80
	CF_4	15	12	0.80
	C_2F_4	15	12	0.80

We concluded that these changes in C1s-XPS spectra are induced by X-ray irradiation, which can induce the elimination of halogen atoms [18,19], not by sorption–desorption of gases.

Taking into account the atomic sensitivity factors [20], we estimated the elemental ratios (Table 2). Overall there was no significant difference before and after gas-sorption. However, the carbon ratios slightly increased and the chlorine ratios slightly decreased due to gas-sorption. These changes are in accordance with the observations of changes in the features of the C1s-XPS spectra [Figs. 2(a) and (b)], which show an increase in the signal intensity of the carbon-rich moieties (appear at lower binding energies) due to gas-sorption. These findings support our expectation that PCTFE films can reversibly adsorb/absorb and desorb solute gases without significantly changing their molecular structure. This led us to study the use of plasma organic films as chemical-sensing layers. They seem promising because the structure of plasma polymer films can be easily modified by varying the plasma conditions (source material, electrical power, pressure, discharge frequency, deposition geometry, etc.).

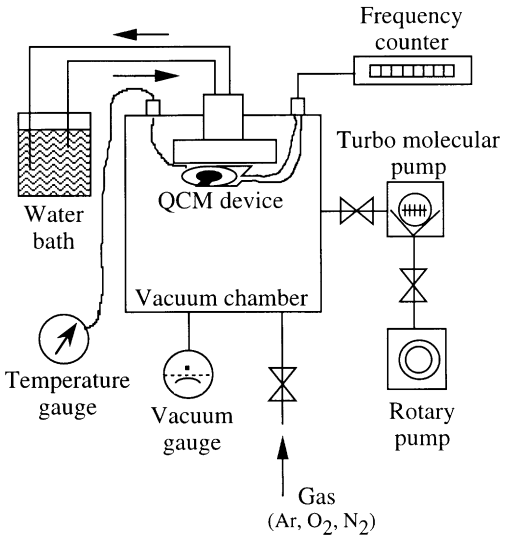

Fig. 3. Gas-sorption measuring apparatus in vacuum condition.

We measured the basic gas sorption capacities of plasma polymer films by the QCR method. We used a vacuum chamber (Fig. 3) in which we could precisely control the temperature and pressure. We measured the sorption capacities of conventional PCTFE film and of amino acid films for Ar, O_2, and N_2 gases. The sorption capacities were determined from the shift in the film-coated QCR following gas exposure.

Prior to sorption measurements, we evacuated the vacuum chamber with steep reduction of resonance frequencies of film-coated QCRs until the minimum pressure at about 1×10^{-6} Torr. The resonance frequencies of all film-coated QCRs were almost constant in a high-vacuum condition. Comparing in an ambient condition, the decrease of resonance frequencies of QCRs in a high vacuum were 5687 Hz for D-tyrosine film, 4140 Hz for D-phenylalanine film, 4037 Hz for D-alanine film, 5568 Hz for D-glutamic acid film, and 197 Hz for PCTFE film.

After the pressure reached 1×10^{-6} Torr, each gases was introduced until the pressure reached 760 Torr; this situation was maintained overnight. As shown in Fig. 4, the introduction of gas created a larger frequency shift for the amino acid films (as indicated by their large sorption capacity) than for the PCTFE film. For all of the films, the highest capacity among the treatment sorption gases was for Ar, probably due to its larger Ostwald coefficient [6] in the LSERs. The validity of LSERs was confirmed by using the amino acid films for 24 VOCs previously [21].

We measured the dependence of the piezoelectric properties of a film-coated QCR on pressure and temperature. In addition to the conventional PCTFE film, we used the amino acid (D-phenylalanine) film for reference. The upward frequency shifts induced by a transfer from an ambient to a high-vacuum (8×10^{-7} Torr) condition were 255 and 1874 Hz for the PCTFE and D-phenylalanine films, respectively. The composition of residual gas determined by a

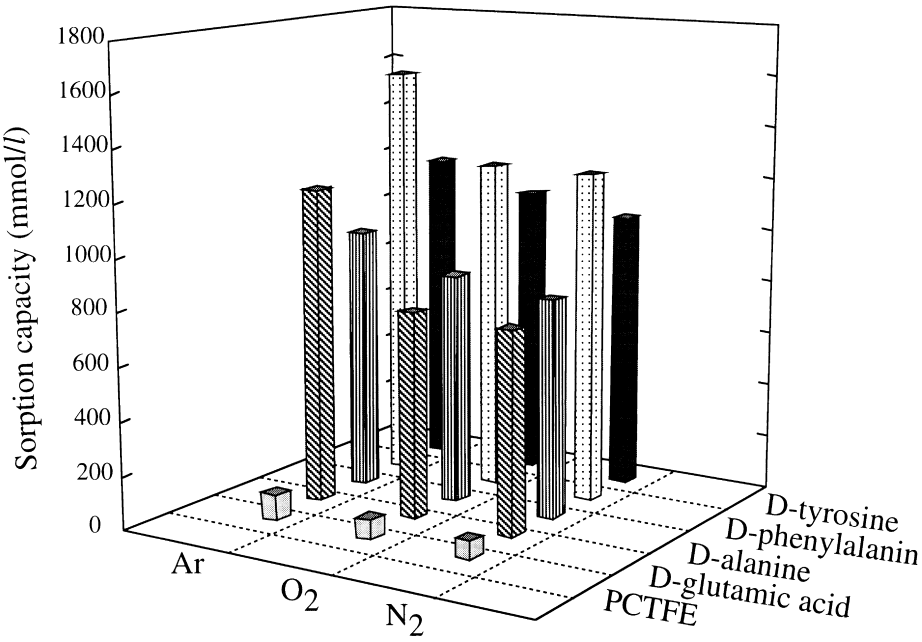

Fig. 4. Sorption capacities of plasma polymer films for pure Ar, O_2, and N_2.

quadrupole mass analyzer was N_2:O_2:$H_2O = 11:5:84$ in the vacuum chamber at 5×10^{-5} Torr. Prior to the film-coated QCR tests, we had confirmed the independence of resonance frequency of a bare QCR without film-coating over the measured pressures and temperatures.

The dependence of the frequency shifts on the temperature using 16°C as the origin (zero point) is shown in Fig. 5. The pressure ranged from 6.2×10^{-7} to 8.6×10^{-7} Torr over the measurement period. The temperature dependencies of the two films showed opposite tendencies. The PCTFE film had a negative frequency-shift coefficient with temperature, indicating that the resonance frequency decreases with temperature. In contrast, the frequency-shift coefficient with temperature of the D-phenylalanine film was positive.

The dependence of the frequency shift on the pressure using 5.5×10^{-7} Torr as the origin (zero point) is shown in Fig. 6. The temperature was kept at 25°C throughout the measurement period. The frequency shifts of the D-phenylalanine film were too large to be ignored at pressures below 10^{-5} Torr. The resonance frequency of the D-phenylalanine film decreased with the pressure, while the resonance frequency of the PCTFE film decreased only 1 Hz over the measured pressures; i.e. it was virtually unchanged over a wide pressure range. The pressure-independence of frequency shift suggest that residual gas dissolved in PCTFE film is completely desorbed even in a low-vacuum condition at 8×10^{-2} Torr. Taking into account this negligible pressure-dependency of frequency shift, the resonance frequency should decrease with increasing temperature of the PCTFE film due to the damping effect [22–28] in QCR

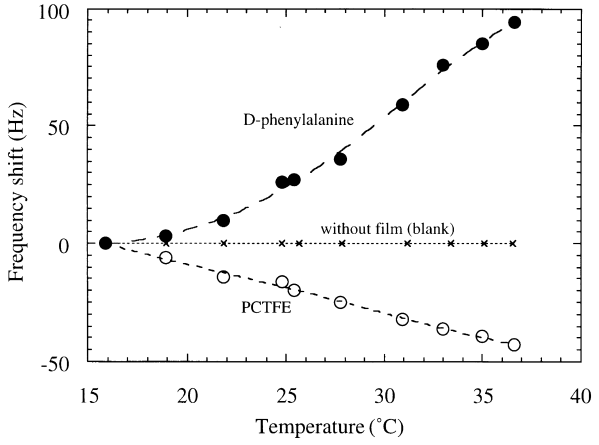

Fig. 5. Frequency shift of film-coated QCR devices for different temperatures in high vacuum.

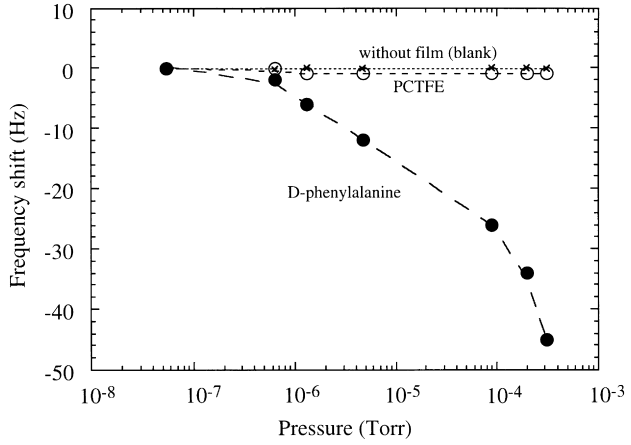

Fig. 6. Frequency shift of film-coated QCR devices for different pressures at constant temperature.

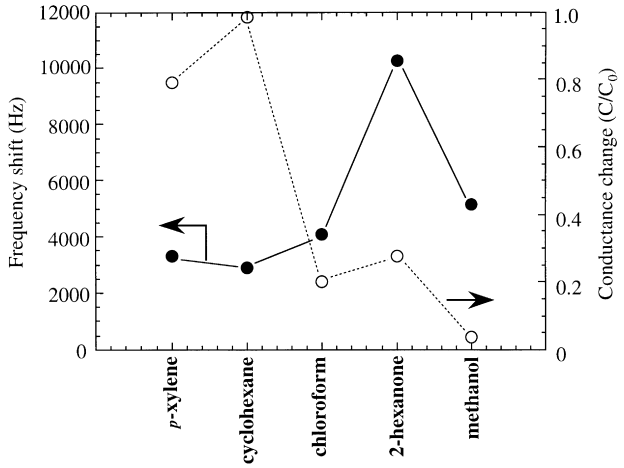

Fig. 7. Frequency shift and conductance change (C_0: conductance before gas sorption; C: conductance when exposed to saturated vapors) of conventional PCTFE-film-coated QCR device.

caused by film-softening. This viscoelastic change is probably induced by the increased temperature effect independent of the residual gas-sorption in the vacuum chamber.

As shown in Fig. 6, the continuous changes of frequency shift depending on pressure for the D-phenylalanine film is confirmed even at an extremely low pressure of 5.5×10^{-7} Torr. This is attributable to the gas liberation from the D-phenylalanine film, indicating the non-equilibrium in gas desorption even in a high vacuum condition. These measurements in a vacuum chamber demonstrated the high sensitivity of a D-phenylalanine-film-coated QCR as a mass balance. This result suggests that D-phenylalanine film has great potential in sorption media even in a high vacuum condition.

As described above, the mechanical properties of the PCTFE film may be changed by its swelling and softening induced by gas-sorption. To clarify this mechanical change, the impedance analysis [24] was implemented by using a network/spectrum analyzer to examine the damping loss of the PCTFE film caused by sorption of VOCs. A PCTFE-film-coated QCR was placed in a sealed 100 ml flask filled with saturated (ca. 10%) VOC vapors at 25°C. Fig. 7 shows the frequency and conductance changes after 5 h of exposure to several VOCs. For hydrocarbons, such as *p*-xylene and cyclohexane, the conductance changed slightly with rather small frequency shifts in comparison with the polar VOCs (chloroform, 2-hexanone and methanol). In contrast, the polar VOCs induced significant reductions in conductance and considerable shifts in the frequency.

Infrared (IR) and electron spin resonance (ESR) spectroscopies indicated the covalent bond formation of the PCTFE film with 2-hexanone [29]. Using IR spectroscopy, this was ascertained by the appearance of strong signals for the C–H and C=O stretching bands in the PCTFE film, after exposure to saturated 2-hexanone vapor and kept in an ambient overnight to desorb 2-hexanone from the PCTFE film. ESR spectroscopy showed that the reduction of spin density of the PCTFE film treated with 2-hexanone vapor of 1.7×10^{19} spins/cm^3, compared with the untreated PCTFE film of 7.8×10^{19} spins/cm^3. This reduction of spin density also suggests the formation of covalent bonds between the PCTFE film and 2-hexanone.

In VOCs, the systematic structural changes, which perturb the physicochemical parameters, provide information about the determinative factors governing the sorption capacities of solvent films. We measured the sorption capacities for chlorinated ethylenes and benzene-derivatives in

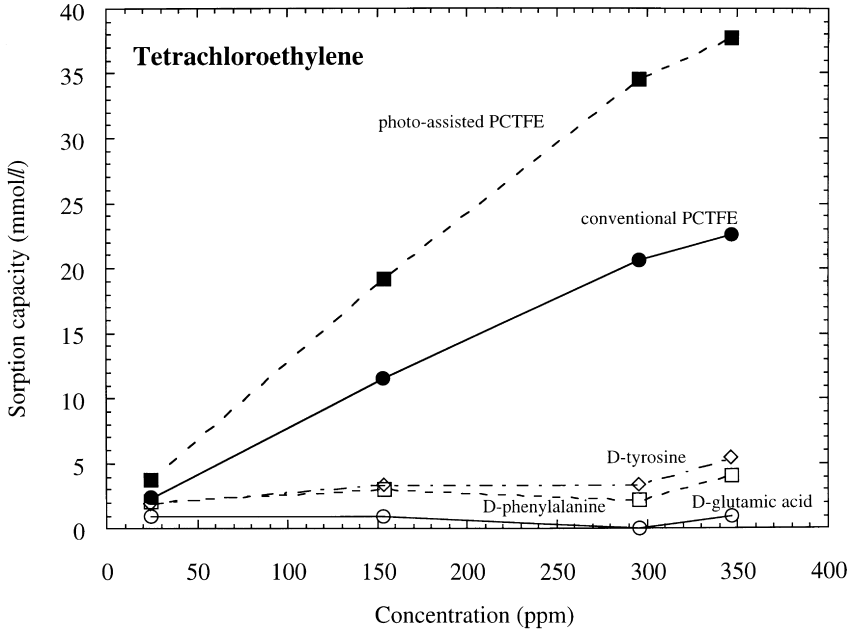

Fig. 8. Concentration-dependent sorption capacities of plasma polymer films for tetrachloroethylene vapors.

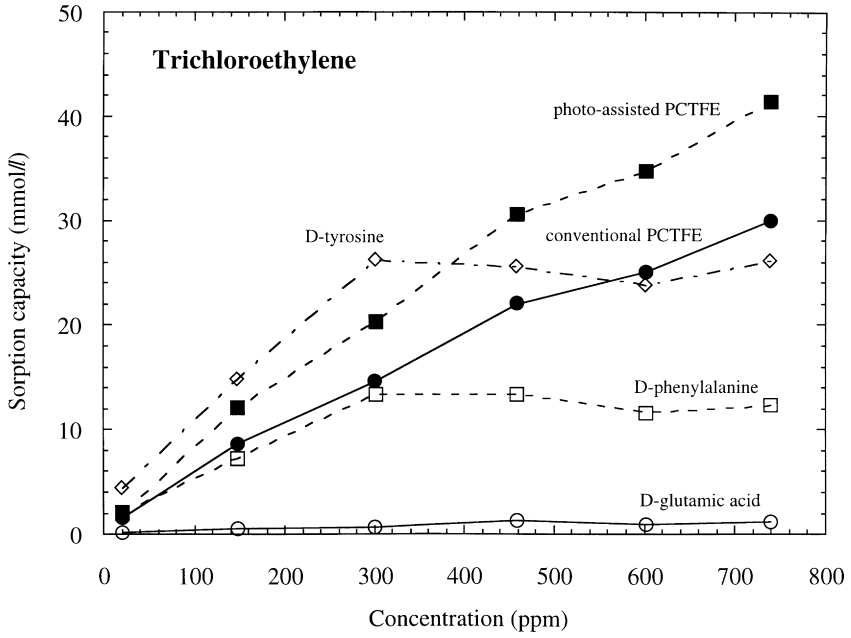

Fig. 9. Concentration-dependent sorption capacities of plasma polymer films for trichloroethylene vapors.

the range of 20–800 ppm as described in the Section 2. In addition to the variation in the sorption capacities of PCTFE films, the variation in the amino acid (D-phenylalanine, D-tyrosine and $_d$-glutamic acid) films are shown in Figs. 8–15. Changing the number of chlorine atoms in chlorinated ethylenes and changing the substituents of the benzene ring change their molecular parameters, enabling us to identify the factors governing the VOC sorption capacities of solvent films.

For both the conventional and photo-assisted PCTFE films, linearity was observed between the vapor concentration and the sorption capacity, obeying Henry's law [30], regardless of the VOC. These observations indicate that the solute molecules of VOC can penetrate into the bulk of the solvent PCTFE films. In contrast, the isothermal sorption curves of amino acid films change irregularly and this irregularity becomes more prominent as the dipolarity of the VOCs decreases (refer to Table 1). Scanning electron microscopy revealed the scattering of crevasses and flakes on the rough surface of amino acid films, suggesting they

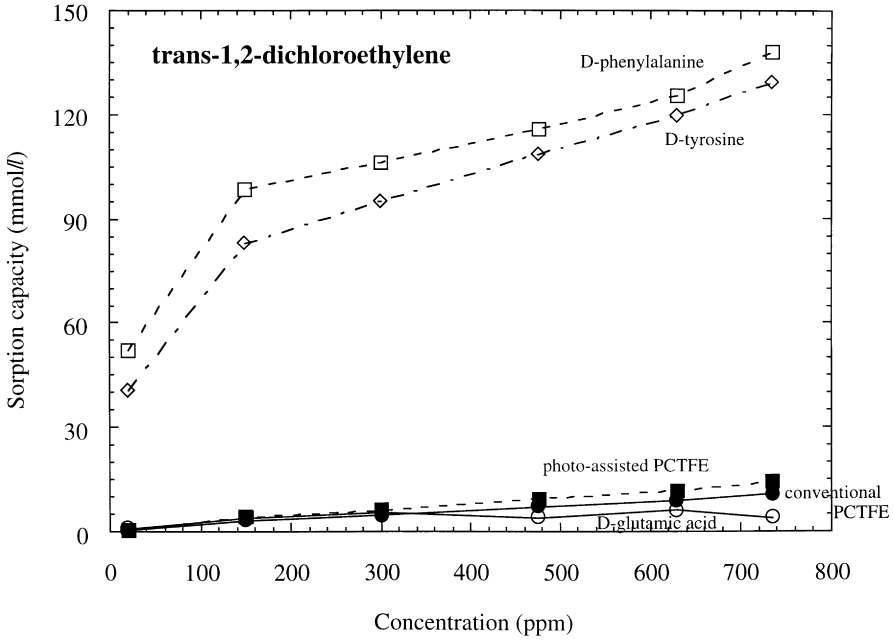

Fig. 10. Concentration-dependent sorption capacities of plasma polymer films for trans-1,2-dichloroethylene vapors.

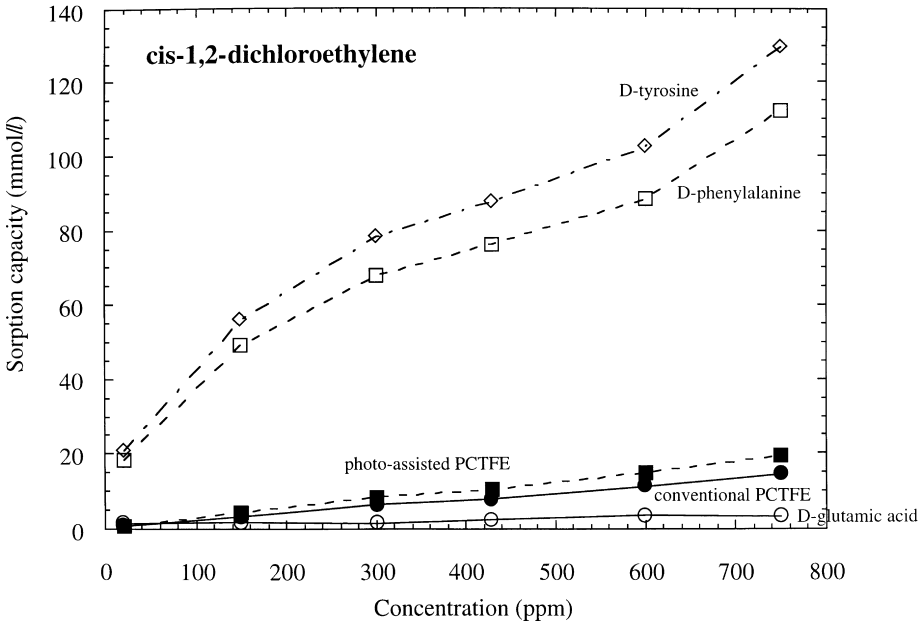

Fig. 11. Concentration-dependent sorption capacities of plasma polymer films for *cis*-1,2-dichloroethylene vapors.

had coarse structure with high surface areas, as shown in Fig. 16. This highly surface-related feature should lead to prominent "surface effects" [31]. The less interactive species, having small dipolarity, are not likely to diffuse into the bulk of the amino acid films after the surface adsorption. This is a plausible explanation for the anomalous sorption behaviors, i.e. not obeying Henry's law, of the amino acid films for non-polar VOCs.

The linearity of the sorption capacities with the vapor concentration for both chlorinated ethylenes and benzene derivatives tends to improve as the dipolarity of the VOCs increases, except for *trans*-1,2-$C_2H_2Cl_2$. This exception may be caused by the local deviation of electrostatic potential on the molecular surface, which can be expressed in some molecular descriptors as local polarity, variability of the surface potential, and electrostatic balance [1]. This enhanced linearity can be interpreted as a bulk effect of solvation due to the intermolecular dipole-interactions, which are stronger than the surface effects in amino acid films. These correlation between concentration and

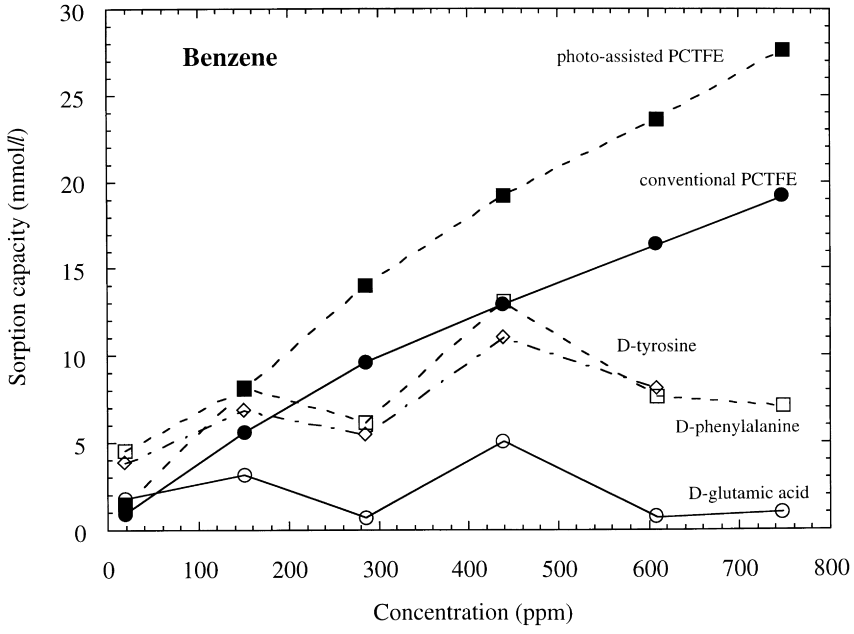

Fig. 12. Concentration-dependent sorption capacities of plasma polymer films for benzene vapors.

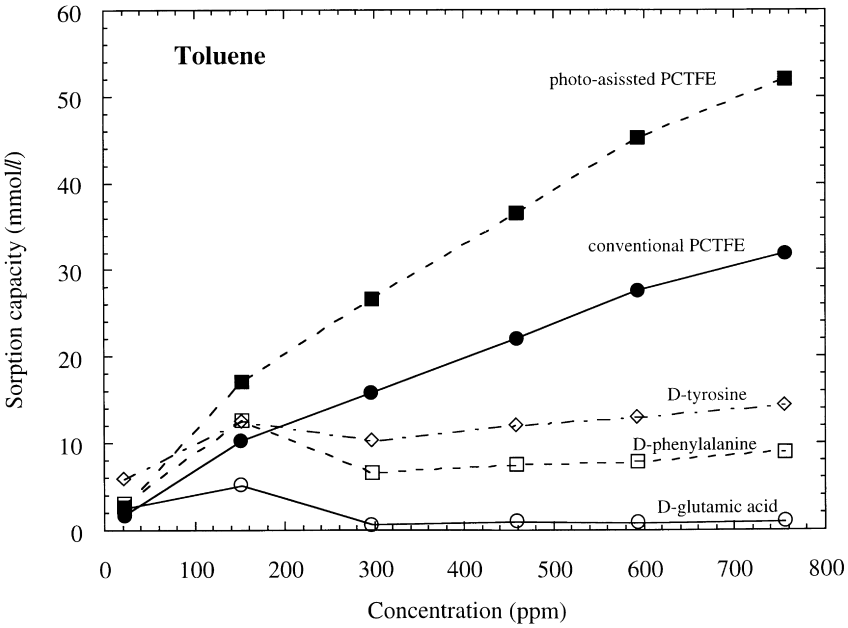

Fig. 13. Concentration-dependent sorption capacities of plasma polymer films for toluene vapors.

frequency shift for similar chlorocarbons were recently reported using siloxane-polymer-coated QCR devices by Zhang and Li [32].

Among the chlorinated ethylenes, conventional and photo-assisted PCTFE films show the highest sorption capacities for C_2Cl_4; their sorption capacities decrease with the number of chlorine atoms. The decreasing chlorine number primarily corresponds to a decrease in polarizability. This polarizability-driven sorption characteristic of PCTFE films is consistent with photo-assisted PCTFE film having higher sorption capacities than conventional PCTFE film over the whole range of measured concentrations. This argument is supported by the finding that the photo-assisted PCTFE film contains large number of unsaturated bonds, which are composed of π-electrons and unpaired electrons and are responsible for polarizability, than the conventional PCTFE film [11].

4. Conclusions

We have reported that the fundamental gas-sorption

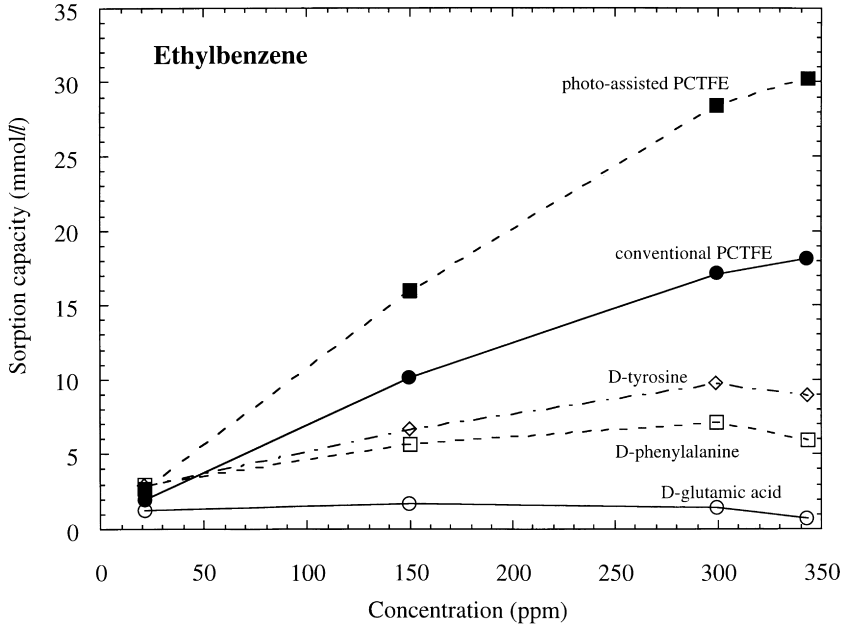

Fig. 14. Concentration-dependent sorption capacities of plasma polymer films for ethylbenzene vapors.

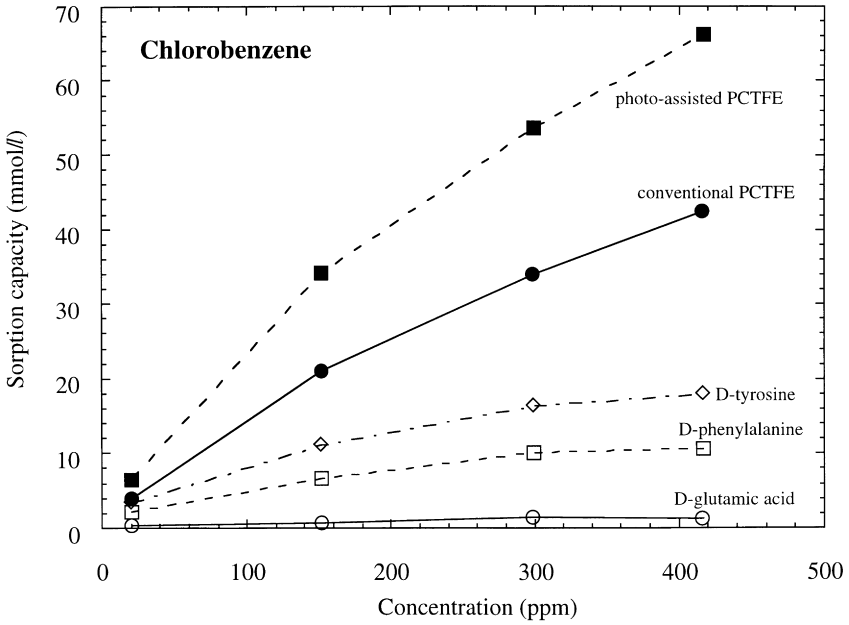

Fig. 15. Concentration-dependent sorption capacities of plasma polymer films for chlorobenzene vapors.

properties of plasma polymer films by using piezoelectric transducer of a quartz crystal resonator as a film substrate. Plasma polymer films were produced by radio-frequency sputtering of polychlorotrifluoroethylene (PCTFE) or amino acids. X-ray photoelectron spectroscopy suggested that the surface molecular structure of the PCTFE film does not change after the sorption of oxygen and fluorocarbon gases. Sorption measurements in a vacuum chamber showed that the PCTFE film completely released the residual gas even at 8×10^{-2} Torr and softened by the increase of temperature whereas the D-phenylalanine film did not completely emit the sorbed gas even at 5.5×10^{-7} Torr. The PCTFE film retains its solvent characteristics without changing its mechanical properties for non-polar organic gases under saturated vapor conditions; however, damping occurs in polar organic gases along with bond formation. The concentration-dependence of sorption capacities for chlorinated ethylenes and benzene derivatives classified the amino acid film as a polar solvent or the PCTFE film as a non-polar solvent.

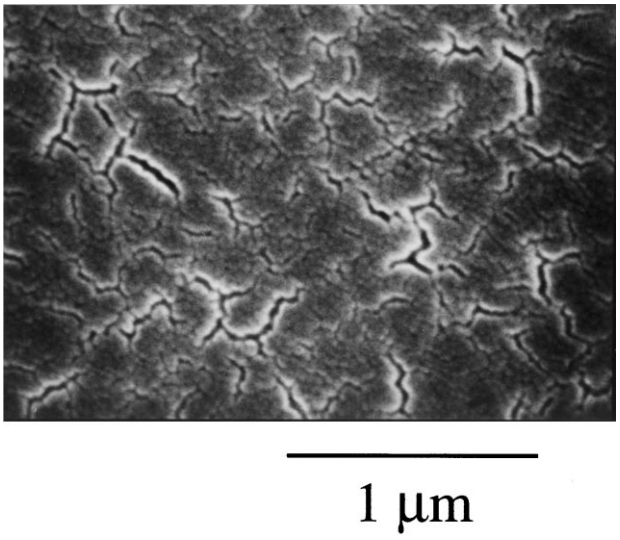

Fig. 16. Surface scanning electron micrograph of the D-phenylalanine film.

References

[1] Hollahan JR, Bell AT. Techniques and applications of plasma chemistry. New York: Wiley, 1974.
[2] Olayan HB, Hamid HS, Owen ED. J Macromol Sci—Rev Macromol Chem Phys 1996;C36:671.
[3] Politzer P, Murray JM. Quantitative treatments of solute/solvent interactions. Amsterdam: Elsevier, 1994.
[4] Grate JW, Abraham MH. Sensors and Actuators B 1991;3:85.
[5] Slater JM, Paynter J. Analyst 1994;119:119.
[6] Abraham MH, Andonian-Haftvan J, Whiting GS, Leo A, Taft RS. J Chem Soc, Perkin Trans II 1994:1777.
[7] Guilbault GG, Jordan JM. CRC Critical Rev in Anal Chem 1988;19:1.
[8] McCallum JJ. Analyst 1989;114:1173.
[9] Sugimoto I, Miyake S. J Appl Phys 1988;64:2700.
[10] Sugimoto I, Miyake S. J Appl Phys 1990;67:2093.
[11] Sugimoto I. Macromolecules 1991;24:1480.
[12] Sugimoto I, Nakamura M, Kuwano H. Anal Chem 1994;66:4316.
[13] Beamson G, Briggs D. High resolution XPS of organic polymers. Chichester: Wiley, 1992.
[14] Sauerbrey GZ. Z Phys 1959;155:206.
[15] Burkert U, Allinger NL. Molecular mechanics (ACS monograph 177). Washington, DC: American Chemical Society, 1982.
[16] Dewer MJS, Zoebisch EG, Healy EF, Stewart JJP. J Am Chem Soc 1985;107:3902.
[17] Weast RC, editor. CRC handbook of chemistry and physics. Boca Raton, FL: CRC Press, 1989.
[18] Wheeler DR, Pepper SV. J Vac Sci Technol 1982;20:226.
[19] Rye RR, Martinez RJ. J Appl Polym Sci 1989;37:2529.

[20] Muilenberg GE, editor. Handbook of X-ray photoelectron spectroscopy. Eden Prairie: Perkin-Elmer, 1979.
[21] Sugimoto I, Nakamur M, Kuwano H. Sensors and Actuators B 1996;35–36:342.
[22] Martin SJ, Frye GC. Proc IEEE Ultrasonics Symp 1991:393.
[23] Hauptmann P, Lucklum R, Hartmann J, Auge J, Adler B. Sensors and Actuators A 1993;37-38:309.
[24] Okajima T, Sakurai H, Oyama N, Tokuda K, Ohsaka T. Electrochimica Acta 1993;38:747.
[25] James D, Thiel DV, Bushell GR, Busfield K, Mackay-Sim A. Analyst 1994;119:2005.
[26] Yin Y, Collins RE. Thin Solid Films 1995;257:139.
[27] Davide FAM, Natale CD, D'Amico A, Hieerlemeann A, Mitrovics J, Schweizer M, Weimar U, Göpel W, Marco S, Pardo A. Sensors and Actuators B 1995;26-27:275.
[28] Rodahl M, Kasemo B. Sensors and Actuators A 1996;54:448.
[29] Sugimoto I, Shimada R. Thin Solid Films 1999, in press.
[30] Suwandi MS, Stern SA. J Polym Sci, Phys Ed 1973;11:663.
[31] Somorjai GA. Chemistry in two dimensions: surfaces. Ithaca, NY: Cornell University Press, 1981.
[32] Zhang S, Li SF. Analyst 1996;121:1721.